

# Supplementary Information: Simulating mesoscale quantum dynamics with an adaptive hierarchy of pure states

Leonel Varvelo, Jacob K. Lynd, and Doran I. G. Bennett\*  
*Department of Chemistry, Southern Methodist University*

## I. HIERARCHY OF PURE STATE (HOPS)

### A. Deriving the normalized non-linear HOPS equation

The non-linear HOPS equation presented in the main text does not match the original version by Suess et al. [2]. The differences result from two changes: first, we ensure that the propagated wave function is normalized at all times, and second, we redefine the hierarchy terms to remove the divergence of their norm with increasing depth of the hierarchy. For completeness, we present the derivation of our equation from the original non-linear HOPS equation given as

$$\begin{aligned} \dot{\psi}_t^{(\vec{k})} = & (-i\hat{H} - \vec{k} \cdot \vec{\gamma} + \sum_n \hat{L}_n \tilde{z}_{t,n}) \psi_t^{(\vec{k})} \\ & + \sum_n \vec{k}[n] g_n \hat{L}_n \psi_t^{(\vec{k}-\vec{e}_n)} - \sum_n (\hat{L}_n^\dagger - \langle \hat{L}^\dagger \rangle_{t,n}) \psi_t^{(\vec{k}+\vec{e}_n)} \end{aligned} \quad (1)$$

where

$$\tilde{z}_{t,n} = z_{t,n}^* + \xi_{t,n} \quad (2)$$

is the shifted noise term and

$$\xi_{t,n} = \int_0^t ds \alpha_n^*(t-s) \langle L_n^\dagger \rangle_t \quad (3)$$

is the time-dependent shift arising from the finite time-scale of reorganization in the thermal environment. As in the main text,  $\alpha_n(t) = g_n e^{-\gamma_n t/\hbar}$  is the correlation function of the thermal environment for the  $n^{\text{th}}$  pigment.

We begin by rewriting the non-linear HOPS equation in terms of new auxiliary wave functions

$$\phi_t^{(\vec{k})} = \frac{\psi_t^{(\vec{k})}}{\sqrt{\langle \psi_t^0 | \psi_t^0 \rangle}} \quad (4)$$

which ensures the true wave function  $\phi_t^{(\vec{0})}$  has a norm of 1 at all times. After taking a derivative and expanding terms, eq. 1 becomes

$$\begin{aligned} \dot{\phi}_t^{(\vec{k})} = & (-i\hat{H} - \vec{k} \cdot \vec{\gamma} - \Gamma_t + \sum_n L_n(z_{t,n}^* + \xi_{t,n})) \phi_t^{(\vec{k})} \\ & + \sum_n \vec{k}[n] g_n(0) \hat{L}_n \phi_t^{(\vec{k}-\vec{e}_n)} - \sum_n (\hat{L}_n^\dagger - \langle \hat{L}^\dagger \rangle_{t,n}) \phi_t^{(\vec{k}+\vec{e}_n)} \end{aligned} \quad (5)$$

where

$$\begin{aligned} \Gamma_t = & \sum_n \langle \hat{L}_n \rangle_t \text{Re}[z_{t,n}^* + \xi_{t,n}] \\ & - \sum_n \text{Re}[\langle \phi_t^0 | L_n^\dagger | \phi_t^{e_n} \rangle] \\ & + \sum_n \langle \hat{L}_n^\dagger \rangle_t \text{Re}[\langle \phi_t^0 | \phi_t^{e_n} \rangle]. \end{aligned} \quad (6)$$

---

\* doranb@smu.edu

is the normalization correction factor.

Second, we correct the norm of the higher order auxiliary wave functions. In their original derivation, Suess et al. [2] noted that the norm of the auxiliary wave functions grows with increasing depth of the hierarchy. Intuitively this is a consequence of the change in units - each step up in the hierarchy represents a higher-order derivative of the true wave function and gains a factor of  $\frac{g_n}{\gamma_n}$  in magnitude. To correct for this we define a new hierarchy  $\tilde{\phi}_t^{(\vec{k})}$ , as

$$\tilde{\phi}_t^{(\vec{k})} = \frac{\phi_t^{\vec{k}_t}}{\prod_n (\frac{g_n}{\gamma_n})^{\vec{k}[n]}} \quad (7)$$

which re-normalizes the auxiliary wave functions to have the same units as the true wave function and ensures that their norm does not diverge with increasing depth. The derivative of  $\tilde{\phi}_t^{(\vec{k})}$

$$\frac{d\tilde{\phi}_t^{(\vec{k})}}{dt} = \frac{d\phi_t^{(\vec{k})}}{dt} / \prod_n (\frac{g_n}{\gamma_n})^{\vec{k}[n]}. \quad (8)$$

is easily evaluated since the normalization is a constant with respect to time. This gives the expression

$$\begin{aligned} \frac{d\tilde{\phi}_t^{(\vec{k})}}{dt} = & (-i\hat{H} - \vec{k} \cdot \vec{w} - \Gamma_t + \sum_n \hat{L}_n(z_{t,n}^* + \xi_{t,n})) \phi_t^{(\vec{k})} / \prod_n (\frac{g_n}{\gamma_n})^{\vec{k}[n]} \\ & + \sum_n \vec{k}[n] g_n \hat{L}_n \phi_t^{(\vec{k}-\vec{e}_n)} / \prod_n (\frac{g_n}{w_n})^{\vec{k}[n]} \\ & - \sum_n (\hat{L}_n^\dagger - \langle \hat{L}^\dagger \rangle_{t,n}) \phi_t^{(\vec{k}+\vec{e}_n)} / \prod_n (\frac{g_n}{\gamma_n})^{\vec{k}[n]} \end{aligned} \quad (9)$$

which we reorganize into the final equation presented in the main text:

$$\begin{aligned} \frac{d\tilde{\phi}_t^{(\vec{k})}}{dt} = & (-i\hat{H} - \vec{k} \cdot \vec{\gamma} - \Gamma_t + \sum_n \hat{L}_n(z_{t,n}^* + \xi_{t,n})) \tilde{\phi}_t^{(\vec{k})} \\ & + \sum_n \vec{k}[n] \gamma_n \hat{L}_n \tilde{\phi}_t^{(\vec{k}-\vec{e}_n)} \\ & - \sum_n (\frac{g_n}{\gamma_n}) (\hat{L}_n^\dagger - \langle \hat{L}^\dagger \rangle_{t,n}) \tilde{\phi}_t^{(\vec{k}+\vec{e}_n)} \end{aligned} \quad (10)$$

where

$$\begin{aligned} \Gamma_t = & \sum_N \langle \hat{L}_N \rangle_t \text{Re}[z_{t,n}^* + \xi_{t,n}] \\ & - \sum_n (\frac{g_n}{w_n}) \text{Re}[\langle \tilde{\phi}_t^0 | \hat{L}_N^\dagger | \tilde{\phi}_t^{e_n} \rangle] \\ & + \sum_n (\frac{g_n}{w_n}) \langle \hat{L}_n^\dagger \rangle_t \text{Re}[\langle \tilde{\phi}_t^0 | \tilde{\phi}_t^{e_n} \rangle] \end{aligned} \quad (11)$$

is changed slightly, and

$$\xi_{t,n} = \int_0^t ds \alpha_n^*(t-s) \langle L_n^\dagger \rangle_t \quad (12)$$

is unchanged from the original definition above.

## B. Short-time correction to the correlation function

The quantum correlation function for the thermal reservoir has a time-reversal symmetry

$$\alpha_n^*(t) = \alpha_n(-t) \quad (13)$$

that, for continuity, implies  $\text{Im}[\alpha_n(0)] = 0$ . When constructing a single exponential description of the correlation function,  $\alpha_n(t) = g_n e^{-\gamma_n t/\hbar}$ , the presence of a non-zero imaginary term in the complex pre-factor ( $g_n$ ) implies  $\text{Im}[\alpha(0)] = \text{Im}[g_n] \neq 0$ . This break-down at short times is usually neglected in such simple descriptions of the correlation function. We have, however, incorporated a second contribution to the correlation function that constructs the correct symmetry property at short-time. Each pigment then has two exponentials composing its correlation function

$$\alpha_n(t) = g_n e^{-\gamma_n t/\hbar} - \text{Im}[g_n] e^{-\gamma_{mark} t/\hbar} \quad (14)$$

where the second term is the short time correction factor that ensures  $\text{Im}[\alpha_n(0)] = 0$ . We set the decay timescale associated with the short-time correction factor ( $\gamma_{mark}$ ) to be substantially faster than the fastest dynamics in the rest of the Hamiltonian. This ensures we can safely approximate this term as a Markovian correction, and, as a result, we do not allow these terms to propagate into the hierarchy. This is accomplished by removing any auxiliary wave function that has a non-zero term associated with a Markovian mode beyond the first-order terms. In the main text we have always described the index vectors in terms of non-Markovian modes and neglected the indices associated with the Markovian modes, since they are a trivial subset of the hierarchy.

### C. Parameters of a HOPS calculation

For the linear chain calculations reported here, the input parameters for a HOPS simulation include: the number of pigments composing the chain ( $N_{pig}$ ), the coupling between nearest-neighbors ( $V$ ), the reorganization energy ( $\lambda$ ) and timescale ( $\gamma$ ) of the Drude-Lorentz spectral density for each pigment, the temperature ( $T$ ), the maximum depth of the hierarchy ( $k_{max}$ ), the integration time step ( $dt$ ), and the total number of trajectories composing the ensemble ( $N_{traj}$ ). We also include one addition timescale ( $\gamma_{mark}$ ) to describe the Markovian mode that provides the short-time correction to the correlation function. For all calculations reported here  $\gamma_{mark} = 500 \text{ cm}^{-1}$  (i.e. a timescale of approximately 10 fs) except for Fig. 3a of the main text where the  $V=250 \text{ cm}^{-1}$  calculations used  $\gamma_{mark} = 1000 \text{ cm}^{-1}$ . Finally, for adHOPS simulations, there is the bound on the derivative error ( $\delta$ ) that is used to define the local basis at each time point.

### D. Sources of error for HOPS calculations

In a HOPS simulation, there are two sources of error for an ensemble averaged property: the statistical error associated with a finite number of trajectories and the hierarchy error arising from a truncation of the hierarchy. In addition to this, there is the time-step error that arises from numerical integration, in this case fourth-order Runge-Kutta.

Here, we characterize the distance between the outcome of two calculations in terms of the mean norm of the population differences

$$\sigma = \frac{1}{N_t} \sum_t \sqrt{\frac{1}{2} \sum_n |\vec{P}_n(t) - \vec{p}_n(t)|^2} \quad (15)$$

where the extra factor of  $\frac{1}{2}$  ensures  $\sigma$  is bounded between 0 and 1.

#### 1. Number of Trajectories

We estimate the statistical error arising from a finite number of trajectories by bootstrapping [1]. We first calculate  $10^4$  trajectories. Then, for each value of  $N_{traj}$  we construct  $10^4$  ensembles by sampling (with replacement)  $N_{traj}$  trajectories from the original ensemble of  $10^4$  trajectories. We use the half-width of the 95% confidence interval to characterize the expected error arising from finite sampling. Specifically, we construct a vector ( $\vec{\Sigma}_t$ ) with half-width of the 95% confidence interval for each site population at a given time ( $t$ ) and estimate the statistical error ( $\epsilon$ )

$$\epsilon = \frac{1}{\sqrt{2}N_t} \sum_t \|\vec{\Sigma}_t\| \quad (16)$$

where the factor of  $\sqrt{2}$  ensures consistency with the error definition. Fig. 1a shows the statistical error as a function of number of trajectories.

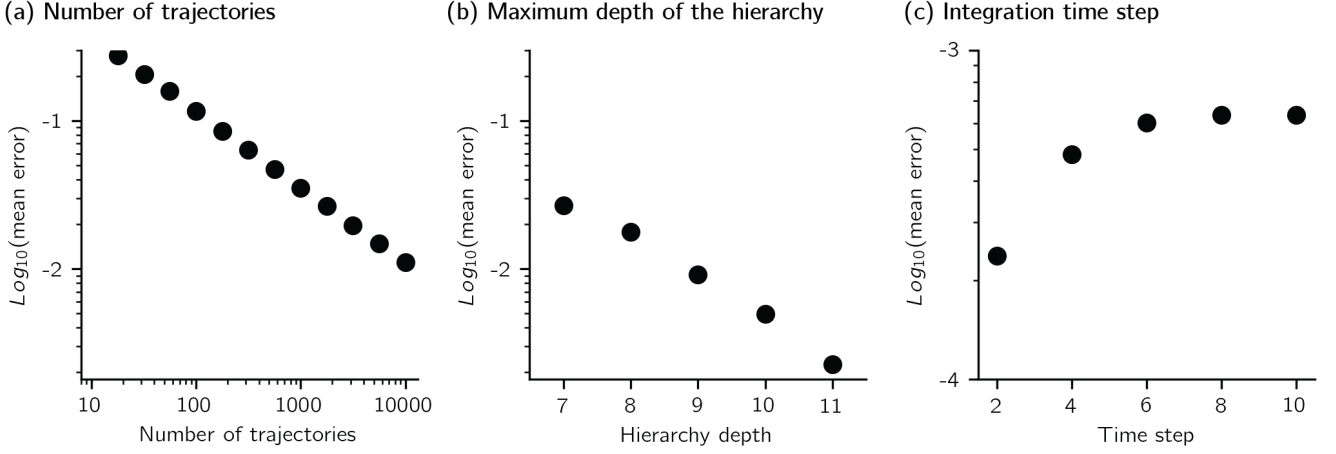


FIG. 1. Comparing error sources in HOPS ensembles. (a) Statistical error from bootstrapping as a function of trajectories with  $k_{max} = 10$ . (b) Error in population vectors as a function of  $k_{max}$  with  $N_{traj} = 10^3$ . (c) Error in population vectors as a function of time step with  $k_{max} = 10$  and  $N_{traj} = 10^4$ . Parameters:  $V = 50 \text{ cm}^{-1}$ ,  $\lambda = 50 \text{ cm}^{-1}$ ,  $\gamma = 50 \text{ cm}^{-1}$ , and  $T = 295 \text{ K}$ .

## 2. Depth of the Hierarchy

HOPS calculations are exact for an infinite hierarchy, but numerical calculations require the calculation to consider only auxiliary wave functions up to some maximum depth ( $k_{max}$ ). To isolate the effects of  $k_{max}$  on the population vectors, we minimize statistical error by performing HOPS calculations at different hierarchy depths with the same noise trajectories. We calculate the error at different depths of the hierarchy by comparing the ensemble average population vector to the results when  $k_{max} = 12$ , using eq. (15). Fig. 1b shows the mean error vs hierarchy depth for  $10^3$  trajectories. By  $k_{max} = 10$  the hierarchy error is comfortably below 0.01, which is used for most of our 5 site calculations.

## 3. Time Step

In numerical integration the time step affects both the accuracy of the trajectory and the computational cost. To test convergence with respect to the time step ( $dt$ ) we consider matched HOPS trajectories with varying  $dt$  values. Figure 1c presents the distribution of mean error (eq. 15) as a function of increasing  $dt$  when compared to population vectors calculated using a time step of 1 fs. The error gradually increases as the time step becomes larger. We did not explore the origin of the integration error, though it is notable that the Markovian mode introduces a timescale of decay that is approximately 10 fs. Except where noted otherwise, we have used a time step of 4 fs which is sufficiently short to sample the Markovian dynamics.

## II. ADAPTIVE HOPS (ADHOPS)

The central result of this work is establishing a time-evolving local basis for the HOPS equation of motion. We define the local basis such that it ensures a selected bound on the derivative error

$$\|D_t - \tilde{D}_t\| \leq \delta \quad (17)$$

where  $D_t$  is the derivative vector calculated in the full basis, while  $\tilde{D}_t$  is calculated in the adaptive basis. For this basis to allow for size-invariant scaling calculations it is essential that the error calculations themselves have local scaling. Below, we

1. evaluate the error terms associated with neglecting elements from either the hierarchy or state basis
2. outline our algorithm for calculating the local basis at each time point
3. discuss the local scaling of error calculations

4. discuss converging calculations with respect to  $\delta$
5. demonstrate how adaptive error is distributed within the ensemble.

### A. Defining the derivative error

Given a current basis for the hierarchy ( $\mathcal{H}_t$ ) and state ( $\mathcal{S}_t$ ) space, we can calculate the error in the derivative induced by neglecting a set of elements in either space at the current time point. We will assume:

1. we have already constructed a derivative operator that acts within the current basis and represent this adaptive derivative operator as  $\frac{\delta_a}{\delta t_a}$
2. the system-bath coupling operators are site-projection operators ( $L_n = |n\rangle\langle n|$ )
3. we can neglect the higher-order error terms arising from the normalization constant  $\Gamma_t$  in eq. (10).

Then the error for neglecting a specific  $\vec{k}$  from the hierarchy basis is given by

$$\Delta_H^2(\vec{k}) = \Theta_{\text{del}}^{(H)}(\vec{k}) + \Theta_{\text{flux-in}}^{(H)}(\vec{k}) + \Theta_{\text{flux-out}}^{(H)}(\vec{k}) \quad (18)$$

where the first term

$$\Theta_{\text{del}}^{(H)}(\vec{k}) = \begin{cases} \sum_{n \in \mathcal{S}_t} \frac{|\psi_{t,n}^{(\vec{k})}|^2}{dt} & \text{if } \vec{k} \in \mathcal{H}_t \\ 0 & \text{otherwise} \end{cases} \quad (19)$$

represents the error arising from assuming the corresponding elements are zero by the end of the next time point. The second term

$$\Theta_{\text{flux-in}}^{(H)}(\vec{k}) = \begin{cases} \sum_{n \in \mathcal{S}_t} \left| \frac{\delta_a \psi_{t,n}^{(\vec{k})}}{\delta t_a} \right|^2 & \text{if } \vec{k} \in \mathcal{H}_t \\ \sum_{n \in \mathcal{S}_t} \left| \frac{g_n}{\gamma_n} N_t^{(\vec{k}+\vec{e}_n)} \psi_{t,n}^{(\vec{k}+\vec{e}_n)} \right|^2 + \left| \gamma_n \vec{k}[n] \psi_{t,n}^{(\vec{k}-\vec{e}_n)} \right|^2 & \text{otherwise} \end{cases} \quad (20)$$

represents the error arising from neglecting flux into the auxiliary wave function, and the final term

$$\Theta_{\text{flux-out}}^{(H)}(\vec{k}) = \begin{cases} \sum_{n \notin \mathcal{S}_t} \left| (\hat{H} \psi_t^{(\vec{k})})_n \right|^2 \\ + \sum_{n \in \mathcal{S}_t} \left| F[\vec{k} - \vec{e}_n] \frac{g_n}{\gamma_n} N_t^{(\vec{k})} \psi_{t,n}^{(\vec{k})} \right|^2 \\ + \sum_{n \in \mathcal{S}_t} \left| F[\vec{k} + \vec{e}_n] \gamma_n (1 + \vec{k}[n]) \psi_{t,n}^{(\vec{k})} \right|^2 & \text{if } \vec{k} \in \mathcal{H}_t \\ 0 & \text{otherwise} \end{cases} \quad (21)$$

represent the error arising from neglecting flux out-of the auxiliary wave function. We have made use of a simple filter function

$$F[\vec{k}] = \begin{cases} 1 & \text{if } \vec{k} \text{ is an allowed auxiliary index.} \\ 0 & \text{otherwise} \end{cases} \quad (22)$$

the ensures that we only consider auxiliary indices that are legal members of the hierarchy (e.g. they do not contain any negative indices).

There is a similar equation for the error induced by neglecting a specific element of the state basis:

$$\Delta_S^2(n) = \Theta_{\text{del}}^{(S)}(n) + \Theta_{\text{flux-in}}^{(S)}(n) + \Theta_{\text{flux-out}}^{(S)}(n) \quad (23)$$

where the deletion error is

$$\Theta_{\text{del}}^{(S)}(n) = \begin{cases} \sum_{\vec{k} \in \mathcal{H}_t} \frac{|\psi_{t,n}^{(\vec{k})}|^2}{dt} & \text{if } n \in \mathcal{S}_t \\ 0 & \text{otherwise} \end{cases} \quad (24)$$

the flux-in error is

$$\Theta_{\text{flux-in}}^{(S)}(n) = \begin{cases} \sum_{\vec{k} \in \mathcal{H}_t} \left| \frac{\delta_a \psi_{t,n}^{(\vec{k})}}{\delta t_a} \right|^2 & \text{if } n \in \mathcal{S}_t \\ \sum_{\vec{k} \in \mathcal{H}_t} \left| (\hat{H} \psi_t^{(\vec{k})})_n \right|^2 & \text{otherwise} \end{cases} \quad (25)$$

and finally,

$$\Theta_{\text{flux-out}}^{(S)}(n) = \begin{cases} \sum_{\vec{k} \in \mathcal{H}_t} \sum_{n' \notin \mathcal{S}_t} |\hat{H}_{n',n}|^2 |\psi_{t,n}^{(\vec{k})}|^2 \\ + \sum_{\vec{k} \in \mathcal{H}_t} \left| F[\vec{k} - \vec{e}_n] \frac{q_n}{\gamma_n} N_t^{(\vec{k})} \psi_{t,n}^{(\vec{k})} \right|^2 \\ + \sum_{\vec{k} \in \mathcal{H}_t} \left| F[\vec{k} + \vec{e}_n] \gamma_n (1 + \vec{k}[n]) \psi_{t,n}^{(\vec{k})} \right|^2 & \text{if } n \in \mathcal{S}_t \\ 0 & \text{otherwise} \end{cases} \quad (26)$$

describes the error associated with neglecting flux out of the  $n^{\text{th}}$  state basis.

### B. Adaptive algorithm

To construct the local basis we determine a set of auxiliary wave functions and states that are sufficient to ensure the derivative error in the adaptive basis is below a given threshold ( $\delta$ ). This is not a uniquely defined basis and the result will depend on the specific algorithm used. Our approach begins by dividing the error into two terms

$$\delta = \sqrt{\delta_H^2 + \delta_S^2} \quad (27)$$

where  $\delta_H$  and  $\delta_S$  are the errors associated with truncating the hierarchy and state basis sets, respectively. In all the calculations presented in this work, we have assumed the error is evenly divided, giving  $\delta_H = \delta_S = \frac{\delta}{\sqrt{2}}$ .

We divide the total basis into four kinds of elements:

1. **stable auxiliary wave functions:** auxiliary wave functions contained in the current basis ( $\vec{k} \in \mathcal{H}_t$ )
2. **boundary auxiliary wave functions:** auxiliary wave functions not in the current basis ( $\vec{k} \notin \mathcal{H}_t$ )
3. **stable states:** state contained in the current basis ( $n \in \mathcal{S}_t$ )
4. **boundary states:** state not in the current basis ( $n \notin \mathcal{S}_t$ )

and we consider these sequentially. We begin with the stable auxiliary wave functions and determine how many can be removed while introducing no more than  $\delta_{H\text{stable}} = \frac{\delta_H}{\sqrt{2}}$  error. We then consider how many boundary auxiliary wave functions must be included to maintain a total hierarchy error  $\sqrt{\delta_{H\text{stab}}^2 + \delta_{H\text{bound}}^2}$  less than  $\delta_H$ . We then perform the analogous operation on the state basis. It is worth recognizing that in the sums over the hierarchy basis in  $\Theta_{\text{del}}^{(S)}$ ,  $\Theta_{\text{flux-in}}^{(S)}$ , and  $\Theta_{\text{flux-out}}^{(S)}$ , we do not need to consider the auxiliary wave functions that have been removed from the basis in the proceeding step because this would double count the associated error.

### C. Size-invariant scaling

One of the essential properties of adHOPS is size-invariant scaling. Once a local basis has been established at each time point, clearly the calculation expense does not depend on the full size of the system. For size invariant scaling, then, it is essential that the calculations required to define the local basis have only local expense.

For a given element of the hierarchy or system basis, calculating the associated error has local expense. In considering eqs. (18)-(26), we note that the only term requiring elements outside of the current basis are of the form  $(\hat{H} \psi_t^{(\vec{k})})_n$ . This term, however, still has local expense as long as the Hamiltonian only supports coupling over a finite spatial extent, such as the usual dipole-dipole coupling which decays with  $\frac{1}{r^3}$ .

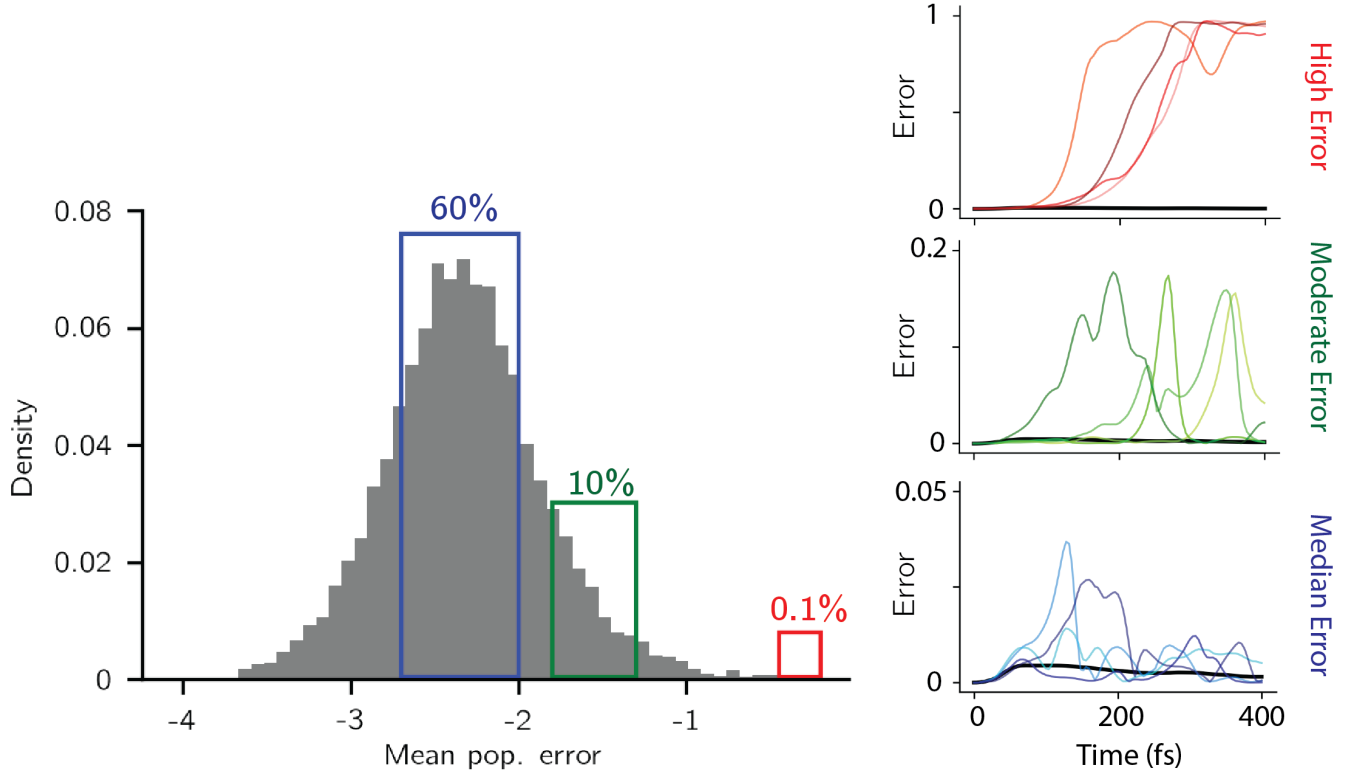


FIG. 2. Population error of individual trajectories and a small ensemble over time. The ensemble contains  $10^4$  matched HOPS and adHOPS ( $\delta = 10^{-3}$ ) trajectories. Population error is root-squared difference. The population error of the ensemble is the mean of the population error of the trajectories. Four high-error trajectories and the ensemble mean are plotted. Parameters:  $V = 50 \text{ cm}^{-1}$ ,  $\lambda = 50 \text{ cm}^{-1}$ ,  $\gamma = 50 \text{ cm}^{-1}$ ,  $T = 295 \text{ K}$ ,  $k_{max} = 10$ ,  $\delta = 10^{-3}$ ,  $N_{traj} = 10^4$ , and  $dt = 4 \text{ fs}$ .

The number of error terms that need to be calculated also has local scaling. On the surface it might appear that a direct calculation of the full error still scales with the system size since the error associated with neglecting each term in the hierarchy and state basis must be considered. However, in most situations, the vast majority of these error terms are zero. For an auxiliary wave function outside of the current basis ( $\vec{k}'$ ) to have a non-zero error term requires that  $\vec{k}' = \vec{k} \pm \vec{e}_n$  for  $n \in \mathcal{S}_t$  and  $\vec{k} \in \mathcal{H}_t$ . For a state ( $n'$ ) outside the current state basis to have a non-zero error requires that  $H_{n',n} > 0$ . Of course, in practice, this is far too generous a bound and the vast majority of states outside of the current basis will have negligible (if not truly 0) coupling. Establishing the limit for coupling to be considered negligible, without needing to be explicitly calculated, is easily (though perhaps not optimally) implemented using a global threshold. More sophisticated approaches require only minimal algorithmic extensions. Taken together, the number of potentially non-zero error terms depends on the size of the current local basis and not the full basis size.

#### D. Derivative error and convergence

In an adHOPS calculations we have two convergence parameters that define the hierarchy basis used across the calculations: the maximum depth of the hierarchy ( $k_{max}$ ) and the bound on the derivative error ( $\delta$ ). We explored the possibility of a coupling between these two convergence criteria that would lead to changes in the converged value of one (e.g.,  $k_{max}$ ) for different values of the other parameter ( $\delta$ ). Our approach starts with a convergence scan for  $\delta$  with values decreasing by logarithmic half-steps (e.g.,  $\log(\delta) = -1, -1.5$ , and  $-2$ ) until the difference between two calculations ( $\sigma$ , eq. (15)) with  $\delta$  separated by 1 log unit was less than 0.01. We then ran a convergence scan for  $k_{max}$  with values increasing by steps of 1 until the difference between two calculations ( $\sigma$ , eq. (15)) with  $k_{max}$  separated by 2 was less than 0.01. We then run a new  $\delta$  convergence scan at the converged value of  $k_{max}$ . In all case we have found this second  $\delta$  scan returns the same convergence value as the first, suggesting that the  $\delta$  and  $k_{max}$  scans are, at least to a first approximation, independent.

### E. Distribution of adaptive error

With the use of an adaptive basis, adHOPS introduces a new form of error into the HOPS framework that arises due to the finite accuracy with which the derivative is calculated at any given time. We calculate the adaptive error for each trajectory in a  $10^4$  member ensemble as the mean difference ( $\sigma$ , eq. (15)) between the equivalent adHOPS and HOPS trajectories. The distribution of adaptive errors (Fig. 2) shows errors spreading more than two orders of magnitude. To explore how error evolves in individual trajectories, we plot the error vs time for trajectories that show extremely high error (red box, red line), moderately high error (green box, green lines), and ‘average’ error behavior (blue box, blue lines). The highest error arises from adHOPS trajectories that diverge from the equivalent HOPS calculations, though these represent around 0.1% of the ensemble. The moderately high errors arise from adHOPS trajectories that show periods in which they drift away from the corresponding HOPS trajectory before returning. The ‘nominal’ error of most adHOPS trajectories show small fluctuations in the vicinity of the corresponding HOPS trajectory. We note that the mean adHOPS ensemble population dynamics are even more similar to the corresponding HOPS calculations than these results suggest due to cancellation of errors. The black line in Fig. 2 shows the error between the ensemble average adHOPS population trajectory compared to the corresponding HOPS ensemble average and has a mean value of  $3 \times 10^{-3}$ .

### REFERENCES

- [1] A. C. Davison and D. V. Hinkley. *Bootstrap Methods and their Application*. Cambridge Series in Statistical and Probabilistic Mathematics. Cambridge: Cambridge University Press, 1997. ISBN: 978-0-521-57471-6. DOI: 10.1017/CB09780511802843. URL: <https://www.cambridge.org/core/books/bootstrap-methods-and-their-application/ED2FD043579F27952363566DC09CBD6A>.
- [2] D. Suess, A. Eisfeld, and W. T. Strunz. “Hierarchy of Stochastic Pure States for Open Quantum System Dynamics”. In: *Physical Review Letters* 113.15 (Oct. 8, 2014), p. 150403. ISSN: 0031-9007, 1079-7114. DOI: 10.1103/PhysRevLett.113.150403. URL: <https://link.aps.org/doi/10.1103/PhysRevLett.113.150403> (visited on 08/10/2020).